

## Epitaxial growth of C<sub>60</sub> thin films on mica

W. Krakow, N. M. Rivera, R. A. Roy, R. S. Ruoff, and J. J. Cuomo  
*IBM T.J. Watson Research Center, Yorktown Heights, New York 10598*

(Received 16 October 1991; accepted 27 November 1991)

Single crystal films of C<sub>60</sub> of different thickness values have been deposited on mica substrates by resistance evaporation. Electron diffraction and high resolution microscopy have been used to assess the orientational ordering and the nature of the defects present in these face-centered cubic films which exhibit a  $\langle 111 \rangle$  direction normal to the film surface.

The ability to be able to fabricate buckminsterfullerenes, C<sub>60</sub> molecules,<sup>1</sup> in reasonably large quantities<sup>2,3</sup> has made possible studies of the structural properties of this form of carbon when it is in a crystalline state. Well-formed three-dimensional bulk crystals up to 0.4 mm diameter have been reported free of solvents using an extraction process, where the C<sub>60</sub> material was heated in a quartz tube and allowed to condense in a cooler region.<sup>4</sup> At room temperature, single crystal x-ray diffraction shows that the molecules are centered on sites of a face-centered cubic (fcc) Bravais lattice, with a high degree of rotational disorder,  $a_0 = 14.2 \text{ \AA}$ . More recently it was also found that a low temperature phase exists below 249 K with diffraction peaks that can be indexed as simple-cubic reflections with mixed odd and even indices (i.e., forbidden reflections<sup>5</sup>). Although somewhat earlier in time, a study of C<sub>60</sub>/C<sub>70</sub> bulk material using electron diffraction and high resolution electron microscopy has revealed a hexagonal close-packed phase which rapidly degraded under the electron beam.<sup>6</sup> Although it was not noted, the reflections can be classified as being of the mixed type. However, because of the appreciable solvent concentration, these forbidden reflections would be caused by localized defects producing void-like regions and hence local regions of simple cubic structure rather than a hexagonal structure.

It is reasonable to expect the highly ordered C<sub>60</sub> thin films will have superior properties to bulk material for certain applications such as superconductivity. To this end, several film studies have been undertaken to understand the early stages of C<sub>60</sub> growth. Monolayer and multilayer growths of C<sub>60</sub> on (110) GaAs at 300 K and elevated temperatures have been studied by scanning tunneling microscopy.<sup>7</sup> Both equilibrium and nonequilibrium structures were found in these van der Waals solids, and there is lack of preference of binding sites on the substrate, except where large corrugations or substrate steps exist. A similar type of study of the monolayer growth regime of sublimed C<sub>60</sub> on mica substrates has also been performed by helium atom scattering.<sup>8</sup> The main conclusion of this work was the demonstration of a single monolayer C<sub>60</sub> epitaxial growth at room tem-

perature conditions with a periodicity of 10.4 Å, which is double that of (001) mica (5.2 Å). Very recently a preliminary investigation of thick film fabrication of C<sub>60</sub> on MoS<sub>2</sub> substrates was reported producing 0.1 μm thick films measuring 1.5 cm × 1.5 cm. Electron diffraction was used and the films were said to be defect-free and monocrystalline.<sup>9</sup>

Along similar lines to the above study, we concurrently have grown thin films of C<sub>60</sub> molecules on (001) mica and NaCl and characterize the film crystallinity and local structural arrangements of the C<sub>60</sub> units. We present here the preliminary results of our electron microscopy examination of thin C<sub>60</sub> films on mica and consider the related defect structures observed in high resolution micrographs.

Commercially purchased carbon soot was extracted with toluene and the C<sub>60</sub> was chromatographically separated, as reported in the literature.<sup>2,3</sup> Mass spectrometry of the powder indicated that no oxygen was bound to the molecules. Films were prepared by loading the pristine C<sub>60</sub> into a resistively heated alumina coated tungsten crucible which was enclosed in an evaporation chamber. The chamber was evacuated by a dry pump reaching a base pressure in the 10<sup>-5</sup> Torr range. The crucible was heated to maintain a deposition rate of about 0.25 Å/s. The chamber pressure remained constant during deposition, indicating that no volatile solvents were present in the C<sub>60</sub> powder. The deposition rate and film thickness were measured by a quartz crystal oscillator calibrated for the deposition geometry used. The substrate temperature was varied in a series of depositions from unheated (RT) to 100, 150, 200, and 250 °C, by use of a quartz radiant heater placed in back of the substrate plate. The substrates employed were 0.75 in. × 0.75 in. muscovite mica, KAl<sub>3</sub>Si<sub>3</sub>O<sub>10</sub>(OH)<sub>2</sub>. The samples were double cleaved to provide clean surfaces on both sides of the sample prior to loading the deposition system. Most films were grown to a thickness of 150 Å except at 200 °C, where 500 Å films were also grown.

For electron microscopy the thin films of C<sub>60</sub> were removed from the mica by lift-off on the surface of water

and mounted on fine 300 or 1000 mesh microscope grids. The microscopy was performed with a JEOL 4000EX microscope operating at 400 kV incident beam energy. The point resolution of this microscope is better than 1.7 Å. Bright-field images were recorded with magnifications up to 300 000 $\times$  with care being taken to avoid any noticeable electron beam damage. Images taken with a minimum dose were unaffected by the electron beam. It was only after prolonged exposure that damage became apparent.

For a substrate temperature of 200 °C, high quality, single crystal C<sub>60</sub> films were obtained on the mica substrates as demonstrated by the diffraction patterns of Fig. 1(a) for a 150 Å thick film and Fig. 1(b) for a 500 Å thickness. The strong first order bulk lattice reflections in (a) are of the {220} type ( $d = 5.0$  Å) which is expected for molecules arranged in a fcc thin film with a [111] normal to the film surface. The next strong Bragg reflections are of the {422} type ( $d = 2.9$  Å). These results are very similar to earlier investigations where metal films were epitaxially deposited on mica at moderate substrate temperatures.<sup>10</sup> The faint innermost reflections in Fig. 1(a) (see arrow), with corresponding spacings of 8.7 Å, appear much sharper than the bulk lattice spots and cannot be indexed in the fcc system since they would have mixed indices. These faint spots occur at the  $1/3\{422\}$  locations which is characteristic of forbidden reflections due to incomplete layer stacking seen in prior studies of fcc metal systems grown in (111) orientations.<sup>11,12</sup> As evidenced in the thicker film diffraction pattern of Fig. 1(b), much weaker  $1/3\{422\}$  reflections are present since the relative diffraction intensity due to incomplete stacking layers is diminished. These reflections should not be confused with a hexagonal lattice, and are present only because excess monolayers occur due to incomplete stacking of bulk layers. These layers, while part of the whole film, individually form a hexagonal two-dimensional net with planar spacings of  $\sim 8.7$  Å.

For other substrate temperatures, both lower and higher than 200 °C, the films on mica tended to be less perfect, exhibiting smaller crystalline domains and more apparent defects. This can be attributed to being in either a three-dimensional growth regime at higher temperatures or to a higher nucleation density at lower temperatures. Cleaved and polished (100) NaCl substrates promoted polycrystalline growth under the conditions where epitaxy was observed on mica. A comprehensive examination of the results will be provided in a later publication.<sup>13</sup> In this report, however, the main focus is on the single crystal films and their fabrication and structural characterization.

The bright-field image of a 150 Å thick (111) single crystal C<sub>60</sub> film grown at 200 °C on mica is displayed in Fig. 2. Here three sets of lattice fringes are present

which are arranged in a hexagonal mesh indicative of the different {220} type reflections producing crossed sets of lattice fringes. The lattice fringe contrast was adjusted by changing the microscope objective lens focus to produce black spot images where the C<sub>60</sub> molecules are located. Because the image is a phase contrast image, it lacks the high contrast typically found by diffraction contrast imaging. However, careful inspection of the

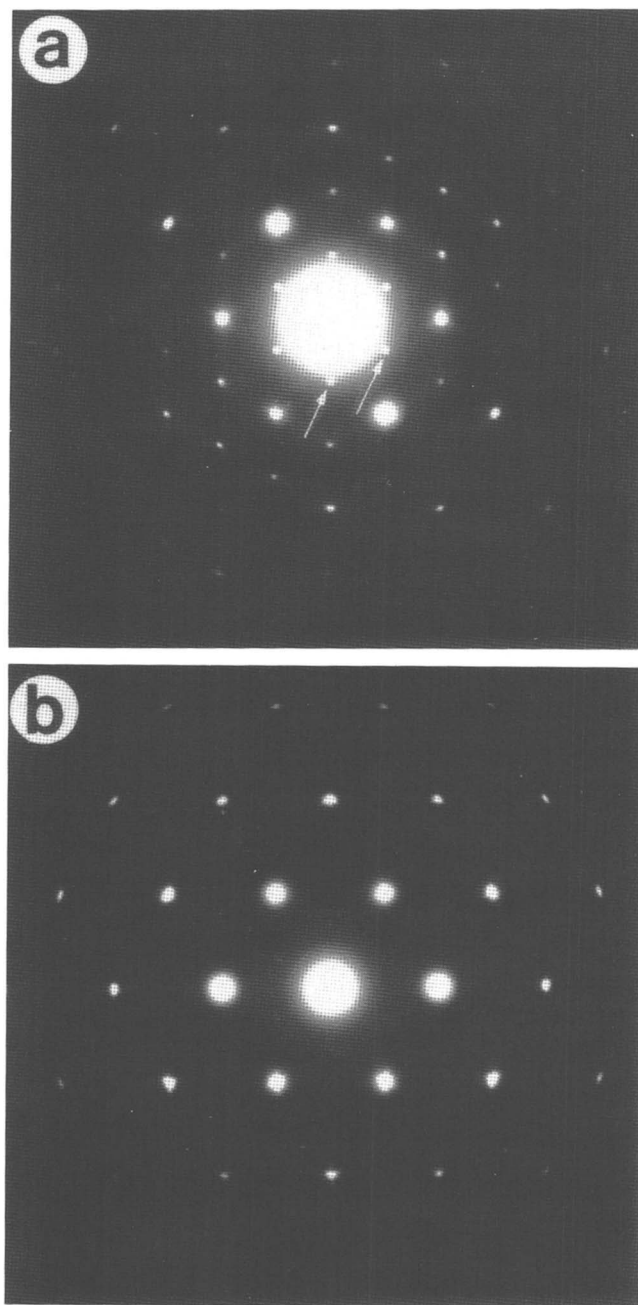


FIG. 1. Electron diffraction patterns of (111) fcc C<sub>60</sub> films on mica: (a) 150 Å film thickness and (b) 500 Å thickness. Arrows indicate some of the forbidden reflections.

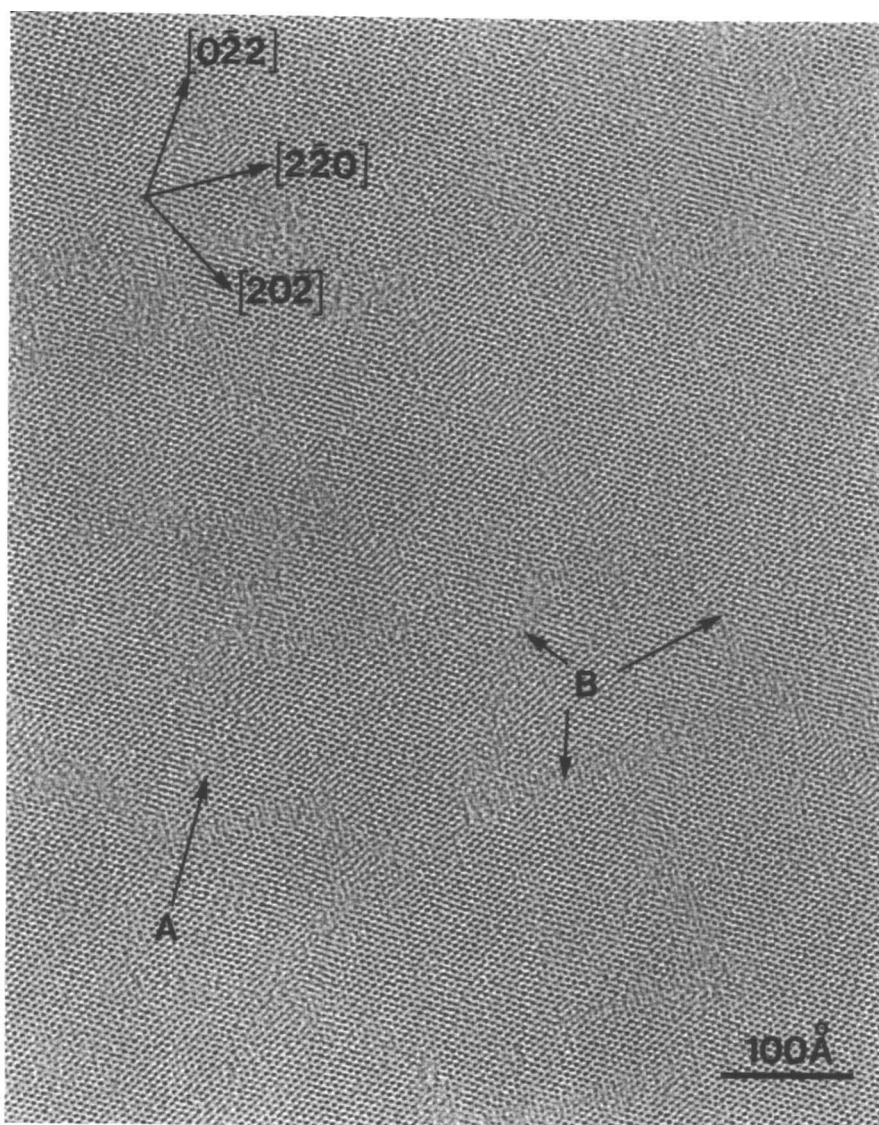


FIG. 2. High resolution bright-field image of a (111)  $C_{60}$  thin film. The direction indicated by an arrow A shows the monolayer lattice of  $\sim 8.2$  Å periodicity. Regions marked B show planar defects inclined to the film plane. Original microscope magnification  $300\,000\times$ .

images reveals that monolayer corrugation periodicities are present when there is incomplete layer stacking. These can be seen by examining the micrograph almost edge-on and viewing along the faint fringe directions. This direction has been labeled by an arrow marked A along one of three possible directions which are rotated by  $\sim 60^\circ$  from a strong bulk lattice fringe direction. It should be noted that these faint fringes are not necessarily continuous owing to the fact that different regions may have different termination layers, i.e., A, B, or C. If an integral number of layers totaling  $3N$  is present, no termination fringes will be visible. Also, we cannot discern whether the excess termination is on the top or bottom surface. This latter point has been explained for thin (111) Au films<sup>12</sup> and the same rules apply to

the thin fullerene films fabricated here. Since the planar spacing of (111) planes is  $8.2$  Å, the total number of layers of fullerenes which form a  $150$  Å thick (111) film is approximately 18. The repeat in the layer sequence ABC... is  $3 \times 8.2$  Å; hence, each column of cluster units visualized in Fig. 2 contains an average of six  $C_{60}$  molecules, i.e., each black dot. It is therefore plausible that a change of one  $C_{60}$  unit in column occupancy would produce a small but visible contrast effect.

Inspection of Fig. 2 also reveals that additional contrast variations are present which tend to follow  $\langle 112 \rangle$  directions and are of finite width, as indicated by several of the regions marked by the letter B. These types of planar defects have also been observed in metals and can be classified as either double positioning

boundaries (DPB) or stacking faults (SF). The double positioning boundaries arise because different regions of the thin film are stacked as ABC..... layers while other regions are stacked in a reversed CBA..... sequence. Here every third plane of the film is continuous across a boundary. The boundary separating these two types of regions usually occurs on  $\{111\}$  planes inclined to the film plane which are at angles of  $70.5^\circ$  to the (111) surface. In addition, coherent (111) twinning plane segments can change the apparent width [see Ref. 12, Fig. 9(c)]. In the case of a stacking fault, the boundary is also on an inclined  $\{111\}$  plane with one part of the crystal being translated with respect to the other by a lattice translation of the type  $\pm 1/3\langle 111 \rangle$ . However, because of the stacking errors in the crystal when these types of boundaries are encountered, SF or DPB, a washing out of the lattice fringes occurs which is just perceptible in the regions labeled B. In other words, the fullerene columns are not aligned in projection above and below the planar defect. For the thicker 500 Å film the defects appear wider and hence cause the images to be more complicated. However, it is believed that the surface topography is similar to the thinner films. Furthermore, these types of defects produce little effect in the diffraction pattern since they arise through simple lattice translations. For somewhat thicker films the diffraction pattern Bragg reflections exhibit Fresnel diffraction streaks which are discernible for the 500 Å case in Fig. 1(b).

Next, the question of lattice mismatch and the planar defect origin can be addressed. Here, the (111) oriented single crystal thin films of  $C_{60}$  have been deposited on muscovite mica and the cleavage plane of mica is defined by the potassium layer sandwiched between two hexagonal sheets of  $SiO_4$  tetrahedra.<sup>14</sup> The in-plane periodicity of these hexagonal arrays is 5.2 Å. A view of the hexagonal layer of tetrahedron units of the mica is shown in Fig. 3. Here  $C_{60}$  units of 10.04 Å diameter are indicated by large circles that have been superimposed to show a likely geometrical correspondence to the mica. It can be seen that the mica can act as a template on a local scale since the mismatch between the mica and  $C_{60}$  radius unit spacings is about 3.4%. This mismatch can readily account for the occurrence of planar defects over a distance of a few hundred angstroms or less. A lattice translation produced by a planar defect for the  $C_{60}$  lattice would maintain the proper coincidence with the underlying mica template.

Finally, we have shown that continuous, single crystal films may be grown over the full dimensions of the mica substrates of 0.75 in.  $\times$  0.75 in. It is expected for a favorable evaporation geometry that this dimension could be extended to several inches on a side since mica sheets are readily available. Thicker films than the 500 Å case reported here could also be grown if

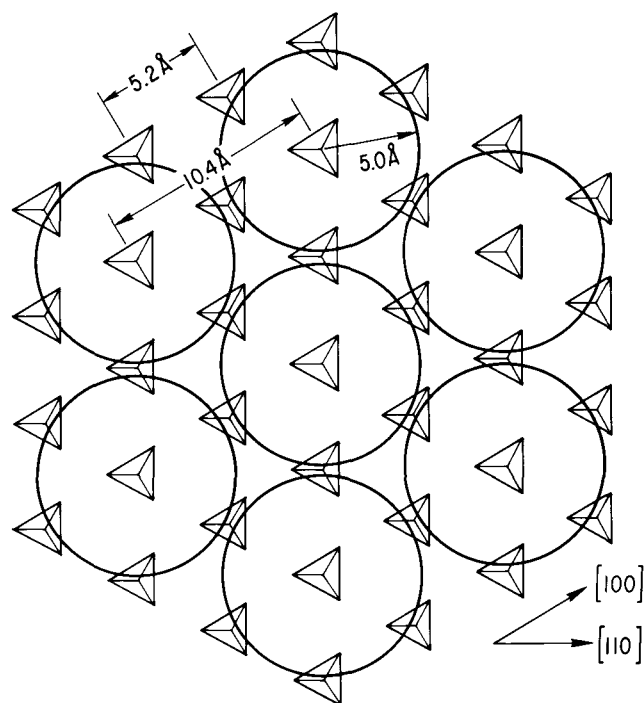


FIG. 3. Schematic view of the mica hexagonal  $SiO_4$  tetrahedron layer and a  $C_{60}$  monolayer. Here a silicon atom is located at the center of each tetrahedron and an oxygen atom at each corner.  $C_{60}$  molecules are depicted as large heavy circles.

it were necessary to have large  $C_{60}$  substrate platforms for chemical experiments or for potential microelectronic circuit fabrication.

## REFERENCES

1. H. W. Kroto, J. R. Heath, S. C. O'Brien, R. F. Curl, and R. E. Smalley, *Nature (London)* **318**, 162 (1985).
2. W. Krätschmer, K. Fostiropoulos, and D. R. Huffman, *Chem. Phys. Lett.* **170**, 167 (1990).
3. W. Krätschmer, L. B. Lamb, K. Fostiropoulos, and D. R. Huffman, *Nature (London)* **347**, 354 (1990).
4. R. M. Fleming, T. Siegrist, P. M. Marsh, B. Hessen, A. R. Kortan, D. W. Murphy, R. C. Haddon, R. Tycko, G. Dabbagh, S. M. Muzsice, M. L. Kaplan, and S. M. Zahurak, *Chem. Comm.* (to be published).
5. P. A. Heiney, J. E. Fischer, A. R. McGhie, W. J. Romanow, A. M. Denenstein, J. P. McCauley, Jr., and A. B. Smith III, *Phys. Rev. Lett.* **66**, 2911 (1991).
6. G. van Tendeloo, M. Op DeBeeck, S. Amelinckx, J. Bohr, and W. Krätschmer, *Europhysics Lett.* **15**, 295 (1991).
7. Y. Z. Li, J. C. Patrin, M. Chander, J. H. Weaver, L. P. F. Chibante, and R. E. Smalley, *Science* **252**, 547 and **253**, 429 (1991).
8. D. Schmicker, S. Schmidt, J. G. Skofronick, J. P. Toennies, and R. Vollmer, submitted to *Phys. Rev. B*, Aug. 8, 1991.
9. A. Koma *et al.*, *Nikkan Kogyo Shimbun*, 8/22/91, p. 6.
10. D. W. Pashley, *Philos. Mag.* **4**, 316 (1959).
11. D. Cherns, *Philos. Mag.* **30**, 549 (1974).
12. W. Krakow, *Thin Solid Films* **93**, 235 (1982).
13. W. Krakow *et al.*, in preparation.
14. R. Elandsson, G. Hadziioannou, C. M. Mate, G. M. McClelland, and S. Chiang, *J. Chem. Phys.* **89**, 5190 (1988).